Analysis of the injection-locked magnetron with a mismatched circulator*

Yue Song(岳 松)[a)b)†], Zhang Zhao-Chuan(张兆传)[a)], and Gao Dong-Ping(高冬平)[a)]

[a)] *Key Laboratory of High Power Micriwave Sources and Technology, Institute of Electronics, Chinese Academy of Sciences, Beijing* 100190, *China*

[b)] *University of Chinese Academy of Sciences, Beijing* 100049, *China*

(Received 6 January 2014; revised manuscript received 18 February 2014; published online 20 June 2014)

Based on the scatter matrix of the four-port lossless mismatched circulator, the phase differential equation of the injection-locked magnetron is derived by comparing different effects of the mismatched and perfect circulator on the injection ratio. Besides, the locking range of the injection-locked magnetron with the mismatched circulator is deduced by functional operation. In addition, the phase differential equation and the locked bandwidth of the injection-locked system with a mismatched circulator are compared with those of the small injection-ratio case with a perfect circulator. The influence of the circulator reflection coefficient on the injection-locked magnetron is also analyzed by numerical calculation. Theoretical analysis shows that the decrement of the locked bandwidth is less than 1% and decrement of the stable phase difference is less than 1.2% when the reflection coefficient is less than 0.1.

Keywords: injection-locked magnetron, mismatched circulator, phase difference, locked bandwidth

PACS: 84.40.Fe, 42.25.Kb, 52.65.Rr **DOI:** 10.1088/1674-1056/23/8/088402

1. Introduction

Microwave tubes are improved to obtain higher powers.[1–5] Among them, the magnetron has been proved to be one of the most efficient and economical industrial microwave generators, which has been widely used in both military and civilian fields.[6] However, the output power of a single magnetron is so limited that it cannot meet the requirements of industrial applications. So it is necessary to perform coherent power-combination by using several magnetrons for higher power microwave output. The precondition of power combination is that the frequencies and phases of these magnetrons accord with each other. The best way to solve this problem is injection-locking an ordinary magnetron, making the output frequency of the magnetron accord with that of the injected signal and getting a stable output phase difference.[7,8]

Injection-locking has been studied theoretically and experimentally for a long time.[9–21] In recent years, the frequency and phase performance of an injection-locked magnetron have been studied in depth.[11,22–24] Adler's condition based on a small injection ratio is widely accepted and adopted by many papers.[12,13,16–19,23] The small injection-ratio solution is derived with a lumped circuit model when the injection ratio is very small. It gives the differential equation of the phase difference between the injected signal and the output signal of the magnetron. Besides, it also shows the relationships between the injection-locked bandwidth and the injection ratio, and between the resonant frequency and the external quality factor of the resonant cavity in the magnetron.[12,13,16–19,23] The large injection-ratio solution predicts a larger injection-locked bandwidth and improves the injection-locked theory.[14]

A circulator separates the injected signal from the output signal of the magnetron, which is necessary in an injection-locked system, so the capability of the circulator has a significant influence on the stability of the injection-locked process. Both the small and large injection-ratio solutions usually are under the assumption of the perfectly matched circulators, which means all ports are matched and there is no reflected wave in the injection-locked system.[9,16] However, mismatching is inevitable for a practical circulator. In this paper we are to theoretically investigate an injection-locked magnetron with a mismatched circulator and to analyze the effects of the mismatched circulator on the phase differential equation and locked bandwidth.

The rest of this paper is organized as follows. In Section 2, both the differential equation and locking range of the injection-locked magnetron with mismatched circulator are derived. Numerical analysis is performed to analyze the effects of reflection coefficient on the injection-locked system in Section 3. Finally, some conclusions are drawn from the present investigation in Section 4.

*Project supported by the National Basic Research Program of China (Grant No. 2013CB328901) and the National Natural Science Foundation of China (Grant No. 11305177).

†Corresponding author. E-mail: yuessd@163.com

© 2014 Chinese Physical Society and IOP Publishing Ltd

2. Theoretical analysis

2.1. Phase differential equation

An injection-locked magnetron system model is shown in Fig. 1. The injected signal source, magnetron, load, and an absorbing load are connected to ports 1, 2, 3, and 4 of the circulator, respectively. The absorbing load is adopted to avoid the effect of the external load on the injected signal source. The arrows show the directions of signal transmission.

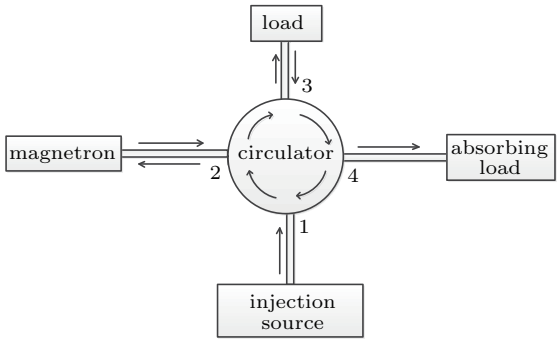


Fig. 1. Configuration of an injection-locked magnetron system with a four-port circulator.

If the circulator is a perfect four-port device, which means it is lossless and mismatching, its scattering matrix can be written as

$$\boldsymbol{S} = \begin{bmatrix} 0 & 0 & 0 & 1 \\ 1 & 0 & 0 & 0 \\ 0 & 1 & 0 & 0 \\ 0 & 0 & 1 & 0 \end{bmatrix}. \tag{1}$$

In the injection-locked system with this ideal circulator, power can only flow from port 1 to port 2, from port 2 to port 3, from port 3 to port 4, and from port 4 to port 1. With the connection shown in Fig. 1, the magnetron and load have no effects on the injected signal source. Meanwhile, the injected signal is isolated from the output signal.

If four ports of the circulator are circularly symmetric, lossless, and mismatched slightly, the corresponding scattering matrix can be written as[25]

$$\boldsymbol{S} = \begin{bmatrix} \Gamma & \Gamma & 0 & 1-\Gamma^2 \\ 1-\Gamma^2 & \Gamma & \Gamma & 0 \\ 0 & 1-\Gamma^2 & \Gamma & \Gamma \\ \Gamma & 0 & 1-\Gamma^2 & \Gamma \end{bmatrix}, \tag{2}$$

where Γ is the reflection coefficient on the circulator port and $|\Gamma| \ll 1$. In order to simplify the analysis and underline the frequency difference between the injected signal and output signal, the reflection coefficient is set to be real.

In the small injection-ratio situation, a lumped circuit model of the magnetron shown in Fig. 2 is adopted.

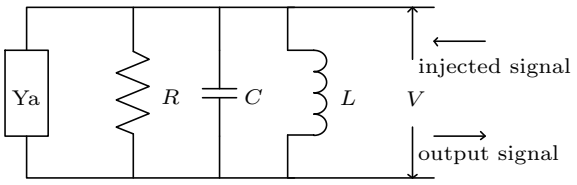


Fig. 2. An equivalent circuit of the magnetron with electronic admittance Ya and passive RLC components.

If the circulator is matched and lossless, the injection ratio is defined as $\rho = V_1 \mathrm{e}^{\mathrm{j}\omega_1 t}/(V \mathrm{e}^{\mathrm{j}\omega t}) = |\rho| \mathrm{e}^{\mathrm{j}\varphi}$, where V_1 is the voltage of the injected signal, ω_1 is its angular frequency, V is the voltage of the output signal of the magnetron, and ω is its angular frequency when an external signal is injected. φ is the total phase difference between the injected signal and the output signal. The angular frequency difference is $\Delta\omega = \omega_1 - \omega$, so the total phase difference is $\varphi = \Delta\omega t + \psi$. ψ is the initial phase difference between the injected signal and the output signal.

The phase differential equation in the small injection-ratio situation is shown as follows:[7,8,11–14,18]

$$\frac{\mathrm{d}\varphi}{\mathrm{d}t} + \frac{\omega_0 |\rho| \sin\varphi}{Q_\mathrm{e}} = \omega_1 - \omega', \tag{3}$$

where ω_0 is the cold cavity resonant frequency of the magnetron, ω' is the angular frequency of the output signal when the magnetron works freely without an injected signal, $|\rho|$ is the amplitude of the injection ratio, and Q_e is the external quality factor of the cavity.

The injection ratio should be modified, if the circulator is mismatched. V_R is the voltage of the load. So there holds $V_\mathrm{R} \approx V S_{32}$, approximately. Since the signal reflected by the load can affect the magnetron, the actual injected signal is the vector synthesis of two components. One part is injected from port 1, whose value is $V_1 S_{21} \mathrm{e}^{\mathrm{j}\omega_1 t}$, while the other part is reflected from port 3, whose value is $V S_{32} S_{33} S_{23} \mathrm{e}^{\mathrm{j}\omega t}$. So the voltage of the total injected signal can be written as $V_i = V_1 S_{21} \mathrm{e}^{\mathrm{j}\omega_1 t} + V S_{32} S_{33} S_{23} \mathrm{e}^{\mathrm{j}\omega t}$.

At this time, the injection ratio of the injection-locked magnetron with the mismatched circulator is

$$\rho_\mathrm{s} = \frac{V_1 S_{21} \mathrm{e}^{\mathrm{j}\omega_1 t} + V S_{32} S_{33} S_{23} \mathrm{e}^{\mathrm{j}\omega t}}{V \mathrm{e}^{\mathrm{j}\omega t}}. \tag{4}$$

If ρ_s is written as $\rho_\mathrm{s} = |\rho_\mathrm{s}| \mathrm{e}^{\mathrm{j}\varphi_\mathrm{s}}$, the amplitude of the injection ratio becomes

$$|\rho_\mathrm{s}| = \sqrt{(|\rho| S_{21} \cos\phi + S_{32} S_{33} S_{23})^2 + (|\rho| S_{21} \sin\varphi)^2}, \tag{5a}$$

and the phase of the injection ratio turns into

$$\varphi_\mathrm{s} = \arctan \frac{|\rho| S_{21} \sin\varphi}{|\rho| S_{21} \cos\varphi + S_{32} S_{33} S_{23}}. \tag{5b}$$

Substituting for the scattering matrix of the mismatched circulator, equations (5a) and (5b) can be written as

$$|\rho_\mathrm{s}| = (1-\Gamma^2)\sqrt{|\rho|^2 + \Gamma^4 + 2|\rho|\Gamma^2 \cos\varphi}, \tag{6a}$$

$$\varphi_s = \arctan \frac{|\rho| \sin\varphi}{|\rho| \cos\varphi + \Gamma^2}. \tag{6b}$$

In practical applications, usually $|\rho| > 0.1$ and $|\Gamma| \ll 1$, so it is reasonable that $\Gamma^2 \ll |\rho|$. Equation (6b) can be simplified into

$$\varphi_s \approx \varphi. \tag{7}$$

The $|\rho|$ and φ in Eq. (3) should be replaced by $|\rho_s|$ and φ_s respectively, when the circulator is mismatched. Then the phase differential equation of the injection-locked magnetron with the mismatched circulator can be written as

$$\frac{\mathrm{d}\varphi_s}{\mathrm{d}t} + \frac{\omega_0 |\rho_s| \sin\varphi_s}{Q_e} = \omega_1 - \omega'. \tag{8}$$

Utilizing Eqs. (6a) and (7), equation (8) can be transformed into

$$\frac{\mathrm{d}\varphi}{\mathrm{d}t} + \frac{\omega_0(1-\Gamma^2)\sqrt{|\rho|^2 + \Gamma^4 + 2|\rho|\Gamma^2\cos\varphi}\sin\varphi}{Q_e} = \omega_1 - \omega'. \tag{9}$$

Equation (9) is the phase differential equation of the injection-locked magnetron with the mismatched circulator. Equation (9) is the same as Eq. (3) when $\Gamma = 0$.

2.2. Locking range

The locking range of the injection-locked magnetron with a mismatched circulator will be deduced as follows.

As soon as the locking is successful, $\mathrm{d}\varphi/\mathrm{d}t = 0$, so there exists

$$\sqrt{|\rho|^2 + \Gamma^4 + 2|\rho|\Gamma^2\cos\varphi}\sin\varphi = \frac{Q_e \Delta\omega_s}{\omega_0(1-\Gamma^2)}, \tag{10}$$

where $\Delta\omega_s = \omega_1 - \omega'$ is defined as the locked angular frequency difference.

Because $\cos\varphi$ is finite, it can be used to deduce the relation between the locked angular frequency difference and the other parameters. Equation (10) can be written as

$$\cos^3\varphi + \frac{|\rho|^2 + \Gamma^4}{2|\rho|\Gamma^2}\cos^2\varphi - \cos\varphi - \frac{|\rho|^2 + \Gamma^4}{2|\rho|\Gamma^2} + \frac{\Delta\omega_s^2 Q_e^2}{2|\rho|\Gamma^2(1-\Gamma^2)^2\omega_0^2} = 0. \tag{11}$$

The magnetron can be injection-locked, if this algebraic equation has a real root.

Replacing x with $\cos\varphi$, equation (11) turns into $x^3 + ax^2 - x - a + b = 0$, where

$$a = \frac{|\rho|^2 + \Gamma^4}{2|\rho|\Gamma^2}, \quad b = \frac{\Delta\omega_s^2 Q_e^2}{2|\rho|\Gamma^2(1-\Gamma^2)^2\omega_0^2},$$

and $x \in [-1, 1]$. A function $f(x) = x^3 + ax^2 - x - a + b$ is constructed to solve the equation for $a, b > 0$. There are some zero points of this function in the interval $[-1, 1]$, when the magnetron can be injection-locked.

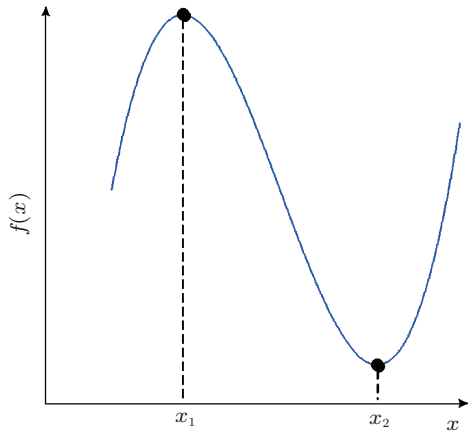


Fig. 3. (color online) Curve of univariate cubic function.

Function $f(x) = x^3 + ax^2 - x - a + b$ is a univariate cubic function and the shape of its curve can usually be drawn as shown in Fig. 3. According to its differential function, $f(x)$ has the extreme point at $x = (-a \pm \sqrt{a^2+3})/3$, but only $x_2 = (-a + \sqrt{a^2+3})/3$ may be in the interval $[-1, 1]$. There is $f(x) > 0$ at the end of the range, because $f(\pm 1) = b > 0$. So the function $f(x)$ must have zero points in the interval $[-1, 1]$, if $f(x_2) \le 0$, there is required that

$$-\frac{2}{27}(a^2+3)^{3/2} + \frac{2}{27}a^3 + b - \frac{2}{3}a \le 0.$$

The inequality can also be written as

$$b \le \frac{2}{3}a - \frac{2}{27}a^3 + \frac{2}{27}(a^2+3)^{3/2}. \tag{12}$$

Utilizing

$$a = \frac{|\rho|^2 + \Gamma^4}{2|\rho|\Gamma^2}$$

and

$$b = \frac{\Delta\omega_s^2 Q_e^2}{2|\rho|\Gamma^2(1-\Gamma^2)^2\omega_0^2},$$

the inequality (12) can be shown as

$$|\Delta\omega_s| \le \frac{\omega_0(1-\Gamma^2)}{Q_e}\left[\frac{2\left(|\rho|^2+\Gamma^4\right)}{3} - \frac{\left(|\rho|^2+\Gamma^4\right)^3}{54|\rho|^2\Gamma^4} + \frac{4|\rho|\Gamma^2}{27}\left(\frac{\left(|\rho|^2+\Gamma^4\right)^2}{4|\rho|^2\Gamma^4} + 3\right)^{3/2}\right]^{1/2}. \tag{13}$$

The inequality (13) shows the locking range of the injection-locked magnetron with a mismatched circulator.

3. Numerical analysis

3.1. Effects of reflection coefficient on locking range

In Section 2, both the differential equation and locking range of the injection-locked magnetron with mismatched circulator have been derived. The reflection coefficient may affect the injection-locked phase. In this section, a numerical analysis based on Eq. (9) and inequality (13) will be performed to analyze how the reflection coefficient affects the injection-locked system.

In the small injection ratio case with a perfect circulator, the locking range of the injection-locked magnetron is $|\Delta\omega_s| \leq \omega_0 |\rho| / Q_e$, so the locked bandwidth of the injection-locked magnetron with a matched circulator in the small injection ratio case is[16]

$$B = \frac{\omega_0 |\rho|}{\pi Q_e}. \tag{14}$$

According to Eq. (13), the locked bandwidth of the injection-locked magnetron with a mismatched circulator is

$$B_s = \frac{\omega_0(1-\Gamma^2)}{\pi Q_e} \cdot \left[\frac{2\left(|\rho|^2+\Gamma^4\right)}{3} - \frac{\left(|\rho|^2+\Gamma^4\right)^3}{54|\rho|^2\Gamma^4} + \frac{4|\rho|\Gamma^2}{27}\left(\frac{\left(|\rho|^2+\Gamma^4\right)^2}{4|\rho|^2\Gamma^4} + 3 \right)^{3/2} \right]^{1/2}. \tag{15}$$

Comparing Eq. (15) with Eq. (14), the bandwidth ratio between these two cases can be shown as

$$\frac{B_s}{B} = (1-\Gamma^2) \left[\frac{2\left(|\rho|^2+\Gamma^4\right)}{3} - \frac{\left(|\rho|^2+\Gamma^4\right)^3}{54|\rho|^2\Gamma^4} + \frac{4|\rho|\Gamma^2}{27}\left(\frac{\left(|\rho|^2+\Gamma^4\right)^2}{4|\rho|^2\Gamma^4} + 3 \right)^{3/2} \right]^{1/2} \Big/ |\rho|. \tag{16}$$

Equation (16) is used for performing numerical calculations to analyze the influences of the reflection coefficient on the locked bandwidth and stable phase difference in a small injection ratio range between 0.1 and 0.4. In practical application, the reflectance is less than -20 dB, so the reflection coefficient should be less than 0.1. Figure 4 shows the relations between bandwidth ratio and injection ratio for $\Gamma = 0.01, 0.05, 0.1$. The relations between bandwidth ratio and reflection coefficient are shown in Fig. 5 for $|\rho| = 0.2, 0.3, 0.4$.

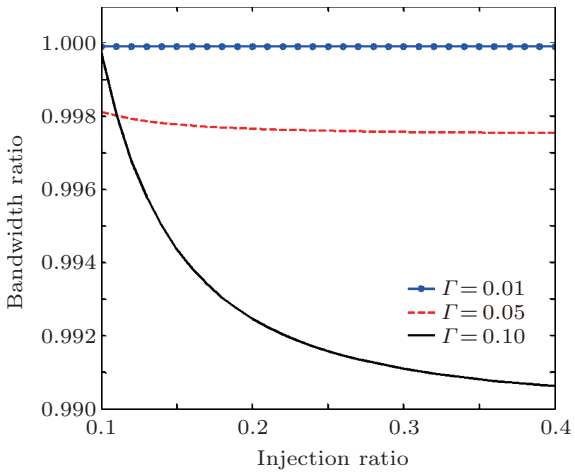


Fig. 4. (color online) Relations between bandwidth ratio and injection ratio for $\Gamma = 0.01, 0.05, 0.1$.

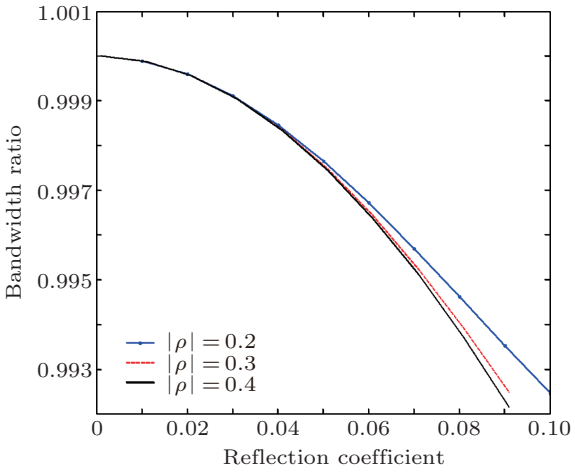


Fig. 5. (color online) Relations between bandwidth ratio and reflection coefficient for $|\rho| = 0.2, 0.3, 0.4$.

As depicted in Fig. 4, the locked bandwidth decreases slightly with the increase of injection ratio. The decrement of the locked bandwidth is less than 1%, when $\Gamma \leq 0.1$ and $0.1 \leq \rho \leq 0.4$. Figure 5 illustrates that the locked bandwidth decreases slightly with the increase of the reflection coefficient. The decrement of the locked bandwidth is less than 1%, when $\Gamma \leq 0.1$ and $0.2 \leq \rho \leq 0.4$. The influence of the reflection coefficient on locked bandwidth may be considered, especially when the injection ratio is a little bigger, if the frequency of the injected signal is at the end of the locked range.

3.2. Effects of reflection coefficient on phase difference

Some parameters of a magnetron are adopted to discuss the effect of the reflection coefficient on the phase difference of the injection-locked magnetron with mismatched circulator.

The cold cavity frequency of the magnetron is 946 MHz. The output frequency of the magnetron is 938 MHz and its external quality factor is 100. It is injected by a 940-MHz signal and the injection ratio is 0.35. The corresponding parameters in Eq. (9) are $\omega_0 = 2\pi \times 946 \times 10^6$ rad/s, $\Delta\omega_s = 2\pi \times (940 - 938) \times 10^6$ rad/s, $|\rho| = 0.35$, and $Q_e = 100$.

The initial value of the phase difference is set to be 0, and these parameters satisfy the locking condition shown in Eq. (13).

The curves of the phase difference versus time are shown in Fig. 6 with Eq. (9), with the values of Γ being 0, 0.05, 0.1.

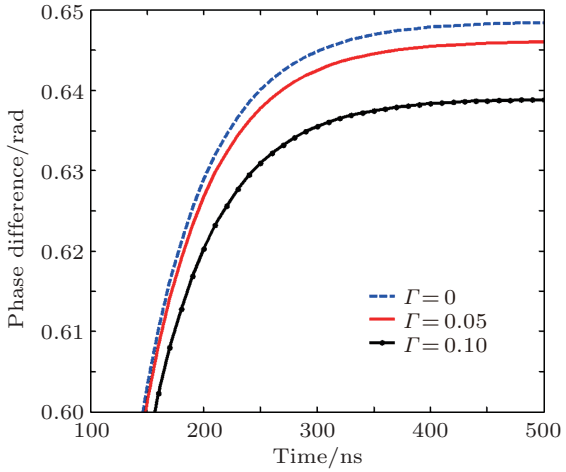


Fig. 6. (color online) Curves of phase difference versus time for three different values of Γ.

The circulator is perfect when $\Gamma = 0$. As can be seen in Fig. 6, the phase difference can eventually reach a steady state when $\Gamma \leq 0.1$. Its stable value decreases slightly with the increase of Γ and the decrement is less than 1.2%. Therefore, the small mismatched degree is allowed in an actual situation. This small reflection coefficient has only a slight influence on phase difference.

In the analysis and calculations mentioned above, the small reflection coefficient has small influences on the injection-locked bandwidth and phase difference of the injection-locked magnetron with a mismatched circulator. Its injection-locked bandwidth and phase difference are very close to those in the perfectly matched case. Therefore, the small reflection coefficient of the mismatched circulator can be neglected and the theory of the injection-locked magnetron with a perfect circulator can be adopted in the actual application. However, in some special cases, for example, if the frequency of the injected signal is at the end of the locked range or the stable phase difference needs to be highly accurate, the effects of the reflection coefficient on the injection-locked bandwidth and phase difference should be considered.

3.3. Effects of port 3 reflection on locking range and phase difference

According to the analysis in Section 2, the total injected signal can be divided into two parts: one part is transmitted from the injection source and the other part is reflected by port 3. The effects of the two parts on the injection-locked system with a mismatched circulator are analyzed. It is obvious that the first part is dominant in the injected signal. Whether the second part reflected by port 3 can be neglected will be analyzed below.

If the reflected signal from port 3 is neglected, then the injected ratio can be written as

$$\rho_1 = \frac{V_1}{V} S_{21}\, \mathrm{e}^{\mathrm{j}\Delta\omega t} = |\rho|\, S_{21}\, \mathrm{e}^{\mathrm{j}\phi} = |\rho|\,(1-\Gamma^2)\,\mathrm{e}^{\mathrm{j}\phi}. \quad (17)$$

According to Eq. (3), the phase differential equation can be written as

$$\frac{\mathrm{d}\varphi}{\mathrm{d}t} + \frac{\omega_0(1-\Gamma^2)\,|\rho|\sin\phi}{Q_\mathrm{e}} = \omega_1 - \omega'. \quad (18)$$

When the reflected signal from port 3 is neglected, the locked bandwidth of the injection-locked magnetron with mismatched circulator can be written as

$$B_1 = \frac{\omega_0(1-\Gamma^2)\,|\rho|}{\pi Q_\mathrm{e}}. \quad (19)$$

A comparison between Eq. (19) and Eq. (14) shows that there exists

$$\frac{B_1}{B} = 1-\Gamma^2. \quad (20)$$

Equation (16) represents the case with the reflected signal from port 3, while equation (20) depicts the case without the reflected signal. The relation between the bandwidth ratio and the reflection coefficient is shown in Fig. 7 for $|\rho| = 0.2$.

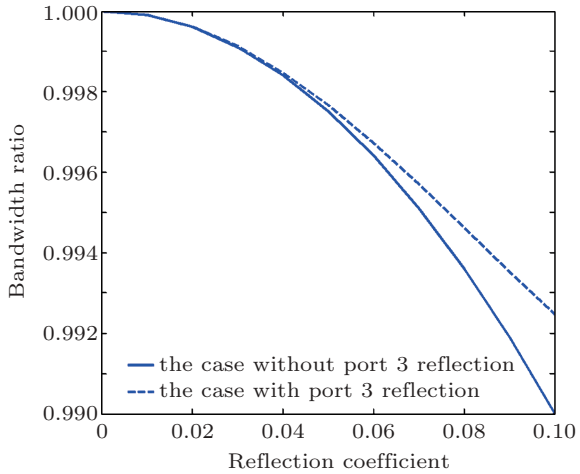


Fig. 7. (color online) Relations between the bandwidth ratio and reflection coefficient with or without the port 3 reflection.

The bandwidth ratio in Eq. (20) is unrelated to $|\rho|$ and it is slightly smaller than that in Eq. (16) with the reflected signal from port 3. So the influence of reflected signal from port 3 on bandwidth ratio can be neglected.

With the same condition, the phase differences depicted by Eq. (18) are shown in Fig. 8 for three different values of Γ.

The stable phase difference increases slightly as Γ increases in Fig. 8, which is opposite to that in Fig. 6. So the reflected signal from port 3 can reduce the stable phase difference. The effects of both the reflection coefficient and port

3 reflection on the stable phase difference may be considered when phase shifter needs to be adjusted accurately in actual application.

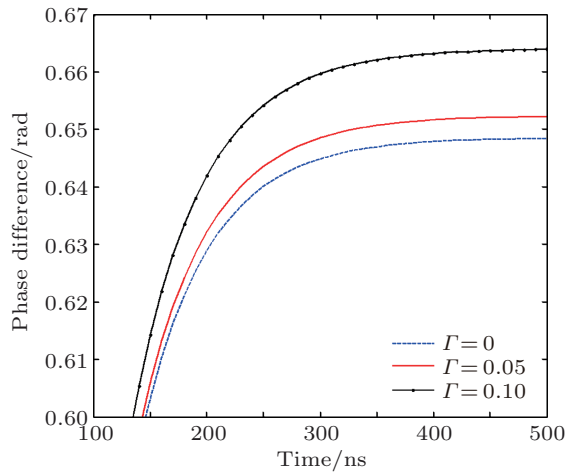


Fig. 8. (color online) Curves of phase difference versus time without the port 3 reflection.

4. Conclusion

The locking range and phase differential equation are numerically calculated and the effect of the mismatched circulator on the injection-locked magnetron system is also analyzed. The results show that the decrement of the locked bandwidth is less than 1% and the decrement of the stable phase difference is less than 1.2% when the mismatch degree is less than 0.1. So the small reflection coefficient of the mismatched circulator can be neglected and the theory of the injection-locked magnetron with a perfect circulator can be adopted in most actual applications. The reflected signal from port 3 can reduce the stable phase difference. However, the influence of the mismatched circulator on locked bandwidth may be considered, if the frequency of injected signal is at the end of the locked range. Besides, the effects of the reflection coefficient on stable phase difference may also be considered when the phase shifter needs to be adjusted accurately in some critical applications.

References

[1] Li W and Liu Y G 2011 *Acta Phys. Sin.* **60** 128403 (in Chinese)
[2] Li W, Liu Y G and Yang J H 2012 *Acta Phys. Sin.* **61** 038401 (in Chinese)
[3] Liu Z B, Huang H, Jin X and Chen H B 2011 *Acta Phys. Sin.* **60** 128402 (in Chinese)
[4] Liu D W, Yuan X S, Yan Y and Liu S G 2009 *Chin. Phys. B* **18** 5507
[5] Xu A, Wang W X, Wei Y Y and Gong Y B 2009 *Chin. Phys. B* **18** 1270
[6] Belanger J M, Jocelyn P J R, Poon O, Fairbridge C, Ng S, Mutyala S and Hawkins R 2009 *The Journal of Microwave Power and Electromagnetic Energy* **42** 24
[7] Song K, Fan Y and He Z 2008 *IEEE Microwave and Wireless Components Letters* **18** 73
[8] DeLisio M P and York R A 2002 *IEEE Transactions on Microwave Theory and Techniques* **50** 929
[9] Shinohara N and Matsumoto H 2008 *IEEE Transactions on Power and Energy* **128** 1119
[10] Choi G W, Kim H J, Kim H J and Choi J C 2008 *IEEE International Vacuum Electronics Conference (IVEC2008)*, April 22–24, 2008, Monterey, CA, p. 445
[11] Tahir I, Dexter A and Carter R 2006 *IEEE Trans. Electron Dev.* **53** 1721
[12] Pengvanich P, Neculaes V B, Lau Y Y, Gilgenbach R M, Jones M C, White W M and Kowalczykd R D 2005 *J. Appl. Phys.* **98** 114903
[13] Razavi B 2004 *IEEE Journal of Solid-State Circuits* **39** 1415
[14] Zhu X Y, Jen L, Liu Q X and Du X S 1996 *Rev. Sci. Instrum.* **67** 2010
[15] Treado T A, Brown P D, Hansen T A and Aiguier D J 1994 *IEEE Trans. Plasma Sci.* **22** 616
[16] Sze H, Smith R R, Benford J N and Harteneck B D 1992 *IEEE Transactions on Electromagnetic Compatibility* **34** 235
[17] Benford J, Sze H, Woo W, Smith R R and Harteneck B 1989 *Phys. Rev. Lett.* **62** 8
[18] Woo W, Benford J, Fittinghoff D, Harteneck B, Price D, Smith R and Sze H 1989 *J. Appl. Phys.* **65** 861
[19] David E E 1961 *Crossed Field Microwave Devices*, Vol. 2 (New York and London: Academic Press) p. 375
[20] David E E 1952 *Proc. Ire* **40** 669
[21] Adler R 1946 *Proc. Ire* **34** 351
[22] Kazakevich G M, Pavlov V M, Jeong Y U and Lee B C 2011 *Nuclear Instruments and Methods in Physics Research Section A: Accelerators, Spectrometers, Detectors and Associated Equipment* **647** 10
[23] Pengvanich P, Lau Y Y, Luginsland J W, Gilgenbach R M, Cruz E and Schamiloglu E 2008 *Physics of Plasmas* **15** 073110
[24] Tahir I, Dexter A and Carter R 2005 *IEEE Trans. Electron Dev.* **52** 2096
[25] Pozar D M, Zhang Z Y, Zhou L Z and Wu D M 2006 *Microwave Engineering*, 3rd edn. (Beijing: Electronics Industry Press) pp. 409–411 (in Chinese) ISBN: 9787121023125